

Correction of the High-Latitude Rain Day Anomaly in the NCEP–NCAR Reanalysis for Land Surface Hydrological Modeling

JUSTIN SHEFFIELD, ALAN D. ZIEGLER, AND ERIC F. WOOD

Department of Civil and Environmental Engineering, Princeton University, Princeton, New Jersey

YANGBO CHEN

Institute of Water Resources and Environmental Engineering, Sun Yat-Sen University, Guangzhou, China

(Manuscript received 19 June 2003, in final form 29 March 2004)

ABSTRACT

A spurious wavelike pattern in the monthly rain day statistics exists within the National Centers for Environmental Prediction–National Center for Atmospheric Research (NCEP–NCAR) reanalysis precipitation product. The anomaly, which is an artifact of the parameterization of moisture diffusion, occurs during the winter months in the Northern and Southern Hemisphere high latitudes. The anomaly is corrected by using monthly statistics from three different global precipitation products from 1) the University of Washington (UW), 2) the Global Precipitation Climate Project (GPCP), and 3) the Climatic Research Unit (CRU), resulting in three slightly different corrected precipitation products. The correction methodology, however, compromises spatial consistency (e.g., storm tracking) on a daily time scale. The effect that the precipitation correction has on the reanalysis-derived global land surface water budgets is investigated by forcing the Variable Infiltration Capacity (VIC) land surface model with all four datasets (i.e., the original reanalysis product and the three corrected datasets). The main components of the land surface water budget cycle are not affected substantially; however, the increased spatial variability in precipitation is reflected in the evaporation and runoff components but reduced in the case of soil moisture. Furthermore, the partitioning of precipitation into canopy evaporation and throughfall is sensitive to the rain day statistics of the correcting dataset, especially in the Tropics, and this has implications for the required accuracy of the correcting dataset. The output fields from these long-term land surface simulations provide a global, consistent dataset of water and energy states and fluxes that can be used for model intercomparisons, studies of annual and seasonal climate variability, and comparisons with current versions of numerical weather prediction models.

1. Introduction

Offline computer simulations of continental- and global-scale water balances are valuable for studying climate variability/change and the hydrological implications thereof. The lack of consistent, long-term observations of land surface water states and fluxes over large spatial scales means that the use of such simulations for determining variability in the major components of the hydrological cycle is an attractive alternative. Conversely, the relative wealth of observations of the atmosphere and sea surface means that a number of global, long-term, near-surface atmospheric analyses exist; for example, the National Centers for Environmental Prediction–National Center for Atmospheric Research (NCEP–NCAR) reanalysis (Kalnay et al. 1996; Kistler et al. 2001), the NCEP–Department of Energy

(DOE) reanalysis (Kanamitsu et al. 2002), and the European Centre for Medium-Range Weather Forecasts (ECMWF) reanalysis (Gibson et al. 1997). These analyses assimilate observed atmospheric and sea surface states into an atmospheric forecast model to obtain global coverage of surface meteorology that can then be used to force land surface models to generate global, sub-daily, datasets of land surface water and energy fluxes and states. Although these model-derived forcing fields may not be perfect, they are self-consistent and are used by many to model the land surface water and energy balances.

The NCEP–NCAR reanalysis provides long-term, near-surface meteorological data (e.g., precipitation, temperature, wind speed, vapor pressure, radiation) at the high temporal resolution (daily and higher) required by land surface models. However, the structure of the atmospheric model used in the reanalysis assimilation system introduces systematic errors into some reanalysis fields, particularly at high latitudes and other regions where observations are scarce. Some analysis variables,

Corresponding author address: Justin Sheffield, Department of Civil and Environmental Engineering, Princeton University, Princeton, NJ 08544.
E-mail: justin@princeton.edu

such as precipitation, are generated entirely by the model without assimilation of observational data and are therefore dependent on the model parameterizations. As such, the precipitation data are acknowledged to be somewhat unreliable at regional and subseasonal scales (Kalnay et al. 1996), although comparisons with independent observations and with several climatologies show that the data contain useful information at seasonal to annual scales (Kalnay et al. 1996; Janowiak et al. 1998; Kistler et al. 2001).

Figure 1 shows the seasonal average number of rain days of the NCEP–NCAR reanalysis for the period 1948–98. At the global scale the spatial patterns of rain days and precipitation seem reasonable with high values in the Tropics that follow the seasonal undulation of the intertropical convergence zone (ITCZ) and lower values in the mid- and high latitudes and the distinctive desert regions in Africa, the Middle East, and Australia, among others. However, a noticeable wavelike pattern (alternating zones of high and low) exists in the high northern latitudes for both the number of wet days and to a lesser extent for the precipitation totals (not shown). This pattern, also reported by Cullather et al. (2000), is most apparent in the winter months of the Northern Hemisphere, reduces somewhat in the spring and autumn, and disappears in the summer months. A similar anomaly, not shown (over ocean), exists in high southern latitudes during the Southern Hemisphere winter.

In this paper the uncertainty in the daily variability of the reanalysis precipitation is assessed by comparison with three other global precipitation datasets: 1) the 15-yr dataset developed by the surface water modeling group at the University of Washington (UW), 2) the 1997–99 Global Precipitation Climatology Project (GPCP) product, and 3) the Climatic Research Unit (CRU) 98-yr dataset. A methodology for correcting the anomaly in the NCEP–NCAR dataset using the monthly statistics from another precipitation dataset is presented. The correction method is applied to the NCEP–NCAR dataset using monthly statistics from each of the three comparison datasets. Motivation for this study is the creation of a global, multidecade, terrestrial, meteorological forcing dataset to drive land surface model simulations of the global water and energy balance. Therefore, the effect of the correction is discussed in terms of the land surface water budget by analyzing long-term simulations using the Variable Infiltration Capacity (VIC) land surface model.

2. Precipitation datasets

a. NCEP–NCAR reanalysis

The NCEP–NCAR reanalysis (referred to hereafter as the NCEP reanalysis) is a retrospective global analysis of atmospheric and surface fields extending from 1948 to the near present (Kalnay et al. 1996, Kistler et al. 2001). Available observations are assimilated into a

global atmospheric spectral model implemented at a horizontal resolution of T62 (approximately 210 km) and with 28 sigma vertical levels. The reanalysis is created using a “frozen” version of the data assimilation system, although assimilated observations are subject to changing observing systems. Consistent gridded output fields are generated continuously in space and time and are classified according to how they are determined and their reliability. Class “A” variables are strongly influenced by assimilated observations and are therefore regarded as being the most reliable fields. These fields include upper-air temperatures, rotational wind, and geopotential height. Less reliable are class “B” variables such as moisture, divergent wind, and surface parameters, which are influenced by observations and the model. Class “C” variables such as surface fluxes and heating rates are completely determined by the model and as such are the least reliable. Precipitation is classified as a class C variable.

b. UW’s daily dataset

The University of Washington surface water modeling group precipitation dataset (Nijssen et al. 2001a) covers a 15-yr (1979–93) time period at 2° resolution. Daily observations from 7800 stations from the Climate Prediction Center (CPC) global dataset are used to downscale the monthly precipitation datasets of Hulme (1995) and the Global Precipitation Climatology Project (Huffman et al. 1997). Aggregation from station data to 2° resolution is carried out using inverse distance square weights based on the distance from each station to the center of each of the 16 0.5° subcells. The final 2° value is the mean of the 16 subcells. In areas where station data are sparse, daily series were generated using a stochastic model consisting of a two-state (wet/dry) first-order Markov chain for precipitation occurrences and a two-parameter gamma distribution for intensities. The parameters are initially estimated from the data derived where station data are available and then interpolated to the data sparse regions.

c. CRU’s monthly dataset

The Climatic Research Unit product is a 0.5° gridded dataset of monthly terrestrial surface climate variables for the period of 1901–98 (New et al. 1999, 2000). The spatial coverage extends over all land areas, including oceanic islands but excluding Antarctica. Fields of monthly climate anomalies, relative to a 1961–90 climatology, were interpolated using thin-plate splines from surface climate data. The anomaly grids are then combined with the 1961–90 climatology resulting in grids of monthly climate over the 98-yr period. Primary variables (precipitation, mean temperature, and diurnal temperature range) are interpolated directly from station observations. The remaining secondary climatic elements (including rain day frequency) are interpolated

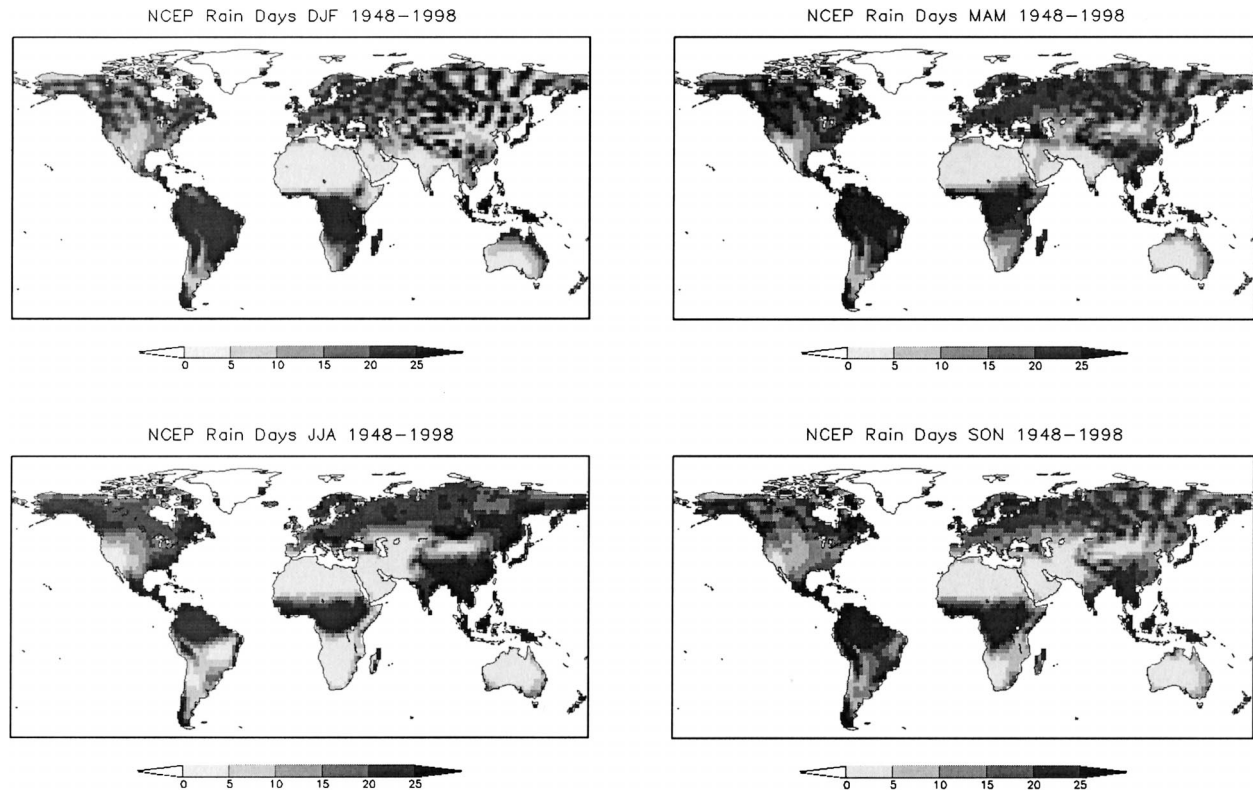


FIG. 1. Seasonally averaged monthly rain days over the period 1948–98 for the NCEP–NCAR reanalysis showing the spurious pattern in the high latitudes of the Northern Hemisphere in the nonsummer months.

from merged datasets comprising station observations and, in regions without station data, synthetic data estimated using predictive relationships with the primary variables.

d. GPCP's daily dataset

The Global Precipitation Climatology Project is a central element of the World Climate Research Program (WCRP 1990; Huffman et al. 1997), providing a daily precipitation product for the period 1997–99 at 1° resolution (Huffman et al. 2001). The data are based on a combination of precipitation estimates from a merged satellite IR dataset over 40°N – 40°S and a rescaling of the Susskind et al. (1997) TIROS Operational Vertical Sounder (TOVS) satellite estimates at higher latitudes. Both contributing estimates are scaled to match the GPCP version 2 monthly satellite–gauge dataset totals (Huffman et al. 1997). Rain day frequencies of the IR-based estimate are adjusted to match data from the Special Sensor Microwave Imager (SSM/I) retrieval. The TOVS-based rain day frequencies are adjusted to the IR-based estimate at 40°N and 40°S separately.

e. Spatial resolution and temporal coverage

To carry out intercomparisons, all datasets were interpolated to a spatial resolution of 2° using bilinear

interpolation over their common spatial coverage of terrestrial areas excluding Greenland and Antarctica. Although previous studies have reported that the high-latitude anomaly in precipitation can be smoothed through interpolation (Cullather et al. 2000; Serreze and Hurst 2000), Fig. 1 shows that the anomaly is still evident in the rain day frequencies after interpolation. There is no single common time period among the four precipitation datasets, so comparison of any two datasets is carried out over their common overlap period. The final corrected precipitation datasets were generated at 2° resolution for 1948–98, this being the common time period of the NCEP and CRU datasets and the CRU dataset being used to scale the corrected precipitation monthly totals as described in section 4.

3. The NCEP–NCAR high-latitude anomaly

The anomaly results from the formulation used for the moisture diffusion in the atmospheric model of the NCEP–NCAR reanalysis system (Kistler et al. 2001; NCEP–NCAR reanalysis information available online at <http://wesley.wwb.noaa.gov/reanalysis.html>). The resulting spurious moisture sink/source creates unrealistically large or small amounts of precipitation and is sensitive to elevation and high latitudes where the specific humidity is low in comparison with the global-average specific humidity. A more accurate approxi-

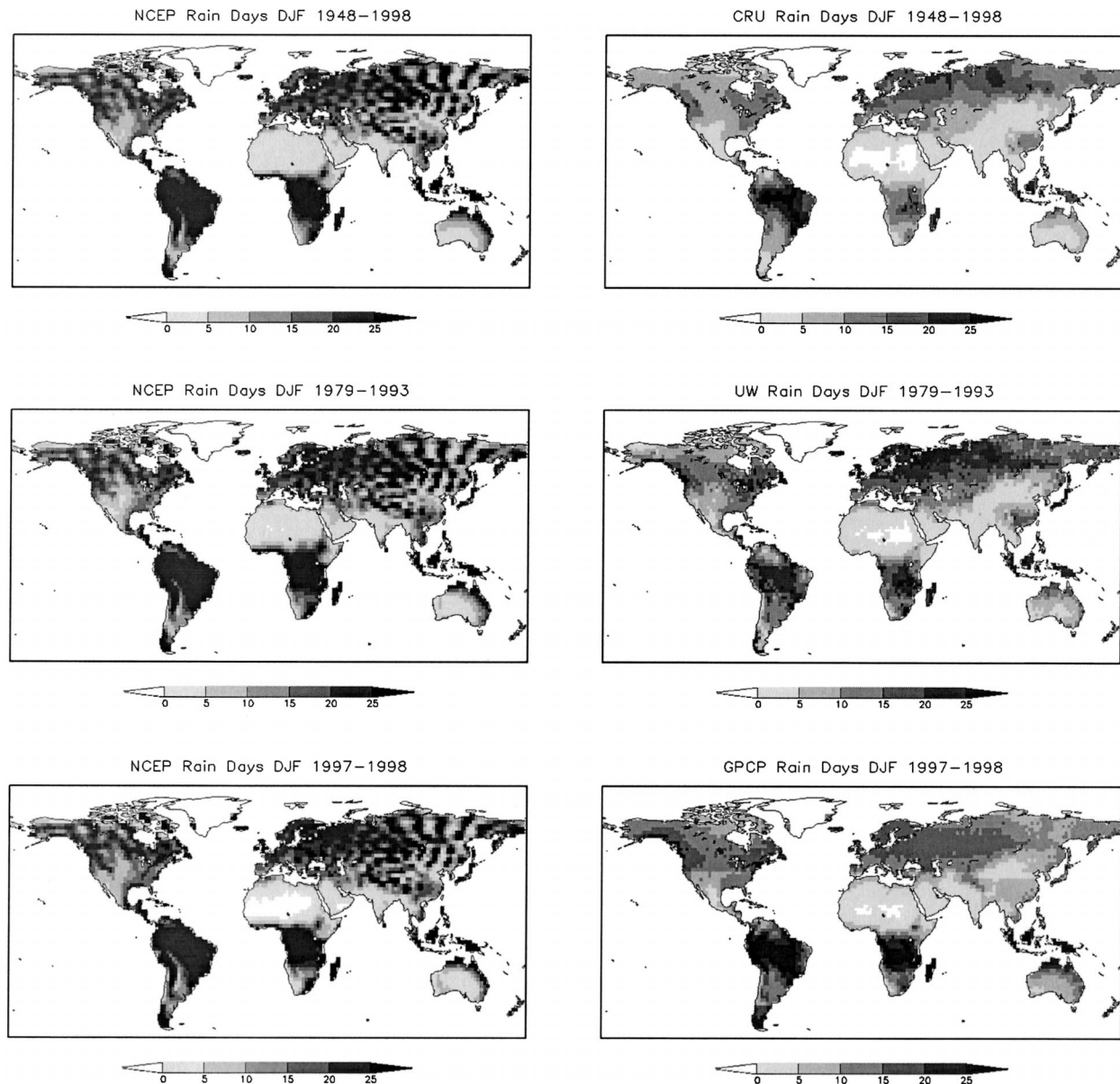


FIG. 2. Seasonally averaged monthly rain days for DJF for (a) the NCEP and CRU datasets for the period 1948–98, (b) the NCEP and the UW datasets for the period 1979–93, and (c) the NCEP and the GPCP datasets for the period 1997–98.

mation of moisture diffusion has been introduced in the next version of the NCEP reanalysis (Kanamitsu et al. 2002), which has corrected the problem. Regardless, the methodology presented in this paper can be applied to this new reanalysis, or any other dataset, to correct any other biases that are revealed.

A comparison of the mean monthly number of rain days of the NCEP reanalysis with the UW, CRU and GPCP datasets is shown in Fig. 2 for the Northern Hemisphere winter months, December–February (DJF). The values are determined for a period of time corresponding to the overlap of the NCEP dataset with the comparison dataset (CRU: 1948–98, UW: 1979–93, GPCP: 1997–

98). From a global perspective, the four datasets are largely similar; however, some important regional differences exist. Most prominent is the high-latitude wavelike anomaly in the NCEP reanalysis. Furthermore, the NCEP reanalysis has more wet days in the Tropics than any of the other datasets, although the GPCP dataset is somewhat similar. The subtropical dry areas compare well between the NCEP reanalysis and each of the other datasets. The high latitudes in the Northern Hemisphere have more wet days in the NCEP reanalysis, most notably in northeast Asia and the northwest and northeast of North America. Similar biases are also evident in all other seasons (not shown), although the high-

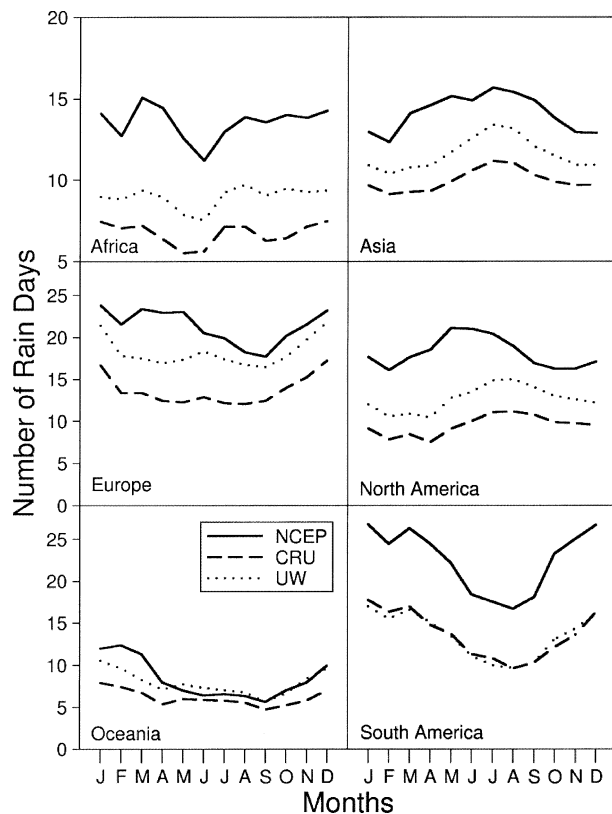


FIG. 3. Time series of average monthly rain days over the period 1979–93 for the continents for the NCEP, CRU, and UW datasets.

latitude wavelike anomaly is not apparent in the Northern Hemisphere summer months.

Figure 3 shows the time series of the mean monthly number of rain days for each continent for the common period of all datasets (1979–93) except for the GPCP dataset, which is not shown as it only overlaps the period 1997–98. In general, the NCEP rain day means are higher than those of the UW dataset, which are in turn higher than the CRU dataset. The exceptions to this are Oceania, for which the NCEP and UW values are similar except for the early part of the year, and South America, where the UW and CRU values match well.

4. Correction of the NCEP reanalysis high-latitude anomaly

a. Correction method

The correction of the anomaly in the NCEP precipitation may be divided into a number of steps: 1) the systematic identification of the grid cells to be corrected, 2) the correction of the NCEP precipitation values for each of these grid cells using the monthly statistics of one of the other precipitation datasets, and 3) scaling of the monthly precipitation totals to match those of the CRU dataset.

1) STEP 1: IDENTIFY THE GRID CELLS TO BE CORRECTED

To decide which grid cells are to be corrected, a statistical test is carried out to determine whether the NCEP dataset is statistically similar to the comparison dataset or not. A Z statistic (based on proportion) is computed for each cell, and this is used to test the null hypothesis that the number of rain days in the NCEP dataset and the comparison dataset are equal. This is repeated for each of the three comparison datasets (CRU, UW, and GPCP). The statistic is calculated based on the total number of rain days for any given month:

$$Z = \frac{p_1 - p_2}{\sqrt{p(1-p)(1/n_1 + 1/n_2)}}, \quad (1)$$

where p_1 is the number of rain days in the NCEP dataset, p_2 is the number of rain days in the comparison dataset, n_1 is the total number of days in the NCEP dataset, n_2 is the total number of days in the comparison dataset, and p is the pooled estimate for the common population proportion:

$$p = \frac{n_1 p_1 + n_2 p_2}{n_1 + n_2}. \quad (2)$$

2) STEP 2: CORRECT THE DAILY PRECIPITATION FOR INCONSISTENT GRID CELLS

The aim of the correction is to force the rain day statistics of the NCEP data to match those of the comparison dataset by using the monthly wet–wet and dry–dry conditional probabilities of the comparison dataset. These probabilities are used within a first-order Markov-type process (Wilks and Wilby 1999) to make decisions on whether the NCEP precipitation on a certain day is of the correct type (wet or dry) in relation to the previous day. The correction algorithm is applied separately for each grid cell and is as follows. To begin, the first day of the NCEP precipitation time series is accepted as being correct. The type of the next day is generated at random using the conditional probabilities of the correcting dataset for the current month and grid cell. If the type of the original NCEP day matches the type of the randomly generated day, then the NCEP precipitation value is accepted. If it does not match, then a day of the appropriate type (wet or dry) is selected at random from the total population of all days of this type in the NCEP dataset for the current month and grid cell. This is repeated for every day in the time series.

The conditional probabilities cannot be calculated for the CRU product, as it is a monthly dataset. Therefore, these are generated by sampling from the archive of UW conditional probabilities for months that have the same rain day frequency as the CRU dataset. For some months, a matching rain day frequency may not exist in the UW archive, so a monthlong time series of wet and dry days was repeatedly generated at random until

it matched the CRU rain day frequency and the conditional probabilities were then calculated from this.

3) STEP 3: SCALE THE MONTHLY TOTALS

Although the correction method described in the previous section ensures that the number of rain days in the NCEP dataset is consistent with the correcting dataset, it ignores the consistency of the precipitation totals. Inconsistent dry days are corrected by replacement with a rain day chosen at random without regard to the precipitation total for the chosen day. This is likely to introduce errors in the monthly precipitation totals that are in addition to the biases that are seen in the precipitation totals of the original NCEP dataset (Trenberth and Guillemot 1998; Kistler et al. 2001). Therefore, in step 3 of the correction method, the NCEP-corrected daily totals are scaled by the ratio of the monthly totals of the CRU and the NCEP-corrected datasets so that the NCEP-corrected monthly totals match those of the CRU dataset. This simple scaling method can potentially produce unreasonably high daily precipitation values when the unscaled daily value is an outlier and the CRU monthly precipitation is much higher than the NCEP precipitation. Such situations are localized and generally occur at the limits of desert regions and at the edge of large-scale climate phenomena with strong seasonal cycles such as the ITCZ. In these regions, relatively small differences between the NCEP and CRU datasets in the location and seasonal variation of these large-scale features can lead to large monthly precipitation ratios at the grid scale. Although the occurrence of unreasonably high daily values is rare and localized, a more robust method of scaling the data to match observed monthly totals would have to be employed in any final version of the corrected dataset.

b. Consistency of related variables

Correcting the precipitation field may result in the related near-surface meteorological variables in the NCEP reanalysis being inconsistent with the corrected precipitation. For example, if a dry day is changed to a wet day, then the original solar radiation for this day may be for a clear day. Therefore, as part of the correction method, the related variables were changed for the same days for which the precipitation was corrected, including wet days that are changed to dry days, ensuring that the dataset is self-consistent.

5. Correction results

The NCEP daily precipitation is corrected with the above methodology using the statistics from each of the three datasets (CRU, UW, and GPCP), resulting in three slightly different corrected precipitation datasets. As the UW and GPCP datasets do not overlap the 1948–98 period completely, the mean monthly conditional prob-

abilities for these datasets are applied repeatedly for all years. This assumes that the mean monthly statistics for the overlap period are representative of the whole 49 years.

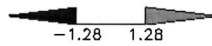
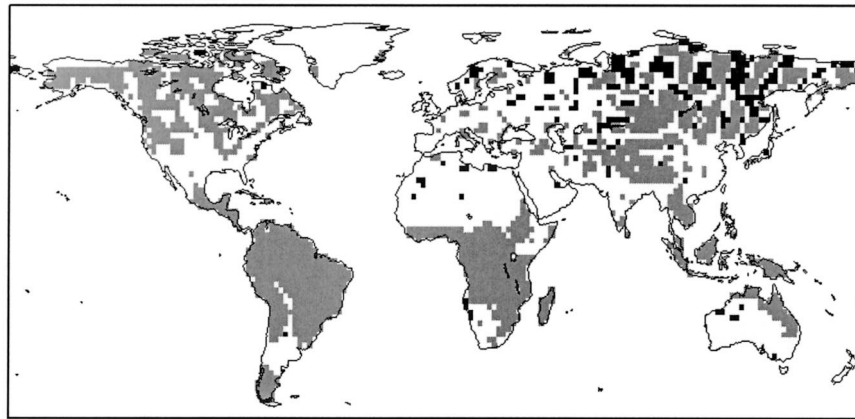
a. Grid cells corrected

The Z statistic was calculated with Eq. (1) for the NCEP dataset and the three comparison datasets over the time periods common to each pair of datasets and an example of the results using the UW statistics are shown in Fig. 4. The unshaded areas indicate where the NCEP data are statistically similar to the comparison dataset. The shaded areas indicate where the NCEP dataset has significantly more (dark gray shading) or less (light gray shading) rain days, based on a 75% confidence level (equivalent to a p value of ± 1.28). It is the data values from these shaded areas that are corrected. The maps highlight the aforementioned differences in rain day frequencies, including the spurious wavelike pattern in the NCEP dataset in the winter months and the significantly higher number of wet days in the NCEP than the UW (and CRU) datasets over much of the globe. The comparison with the GPCP dataset (not shown) shows a closer match in general, which may be due to the GPCP rain days being based on satellite grid values as opposed to gauge data that may tend to underestimate the frequency of rain. However, the short time period (3 yr) of the GPCP dataset results in a weak statistical test and therefore the worth of the comparison is unknown.

b. Corrected datasets

An example of the results of the correction is shown in Fig. 5. This is the seasonally averaged number of rain days for the Northern Hemisphere winter (DJF) for the UW dataset and the corresponding corrected dataset. The corrected precipitation dataset resembles the corresponding correcting dataset, which is desirable and to be expected as the correction method is designed to force the statistics of the two datasets to match. The results for the other seasons and correcting datasets (CRU and GPCP) similarly show good matches. In addition to correcting the high-latitude rain day anomaly, differences that occur elsewhere are also removed. For example, in the Tropics the high numbers of rain days in the NCEP dataset are reduced to the levels found in the CRU and UW datasets. This is illustrated more clearly in Fig. 6, which shows a scatterplot of the NCEP average monthly number of rain days versus that for the CRU, UW, and GPCP datasets and their respective corrected versions for the six continents. The corrected datasets are similar to the corresponding correcting dataset for both the CRU and UW with some slight differences most evident for the UW dataset over Europe and Oceania. In the case of the GPCP dataset, the corrected data are generally closer to the GPCP dataset

Z-statistic NCEP vs UW 1979–1993 January



Z-statistic NCEP vs UW 1979–1993 July

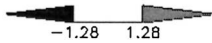
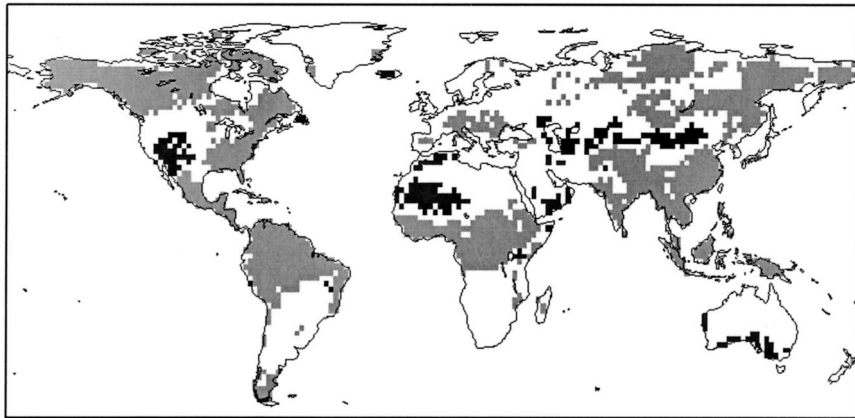


FIG. 4. Global Z statistic [Eq. (1)] indicating the statistical similarity between the mean monthly number of rain days of the NCEP dataset and UW dataset for Jan and Jul. The values of ± 1.28 are the critical levels of the Z statistic in a two-tailed test at a 75% confidence level.

than to the NCEP dataset, yet there are still large differences for most continents. In any case, the monthly statistics of the corrected dataset will never be identical to those of the correcting dataset because of the stochastic nature of the correction method. How well they match depends also on the difference between the NCEP and correcting dataset and the threshold (or confidence level) of the statistical test for determining if a grid cell requires correction.

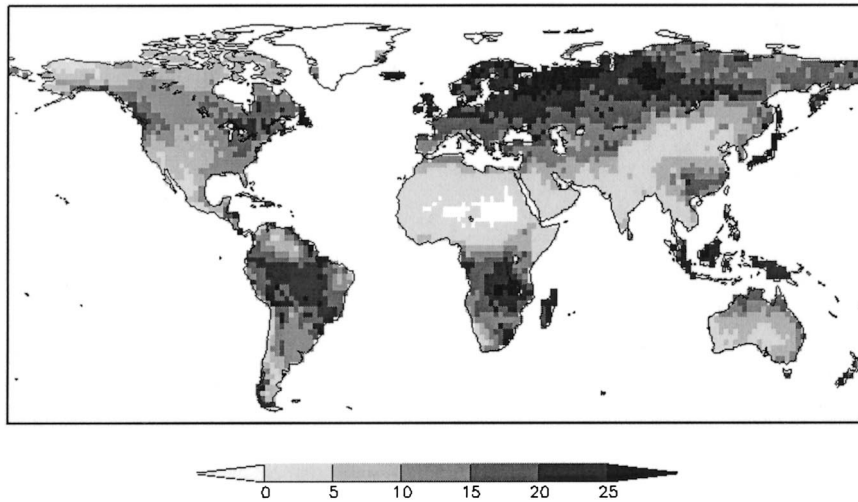
6. Discussion

a. Choice of correcting dataset

The correction method may be applied using the statistics from any dataset and each of the datasets used

here (CRU, GPCP, and UW) may be equally valid for correcting the high-latitude anomaly. However, the methods used to construct each dataset results in differences in the rain day statistics that are regionally and seasonally variable. Deciding on which dataset to use for correcting the NCEP precipitation may be somewhat subjective, but certain factors may influence the decision. The accuracy of the dataset is perhaps of greatest importance and this is highly dependent on the methods and observations used to construct the datasets. The accuracy of the UW and CRU datasets is highly dependent on the density of stations and methods used to interpolate to the grid scale. Low station density will tend to give an underestimation of precipitation occurrence in a grid, especially when convective precipitation

UW Rain Days DJF 1979–1993



UW Corrected Rain Days DJF 1979–1993

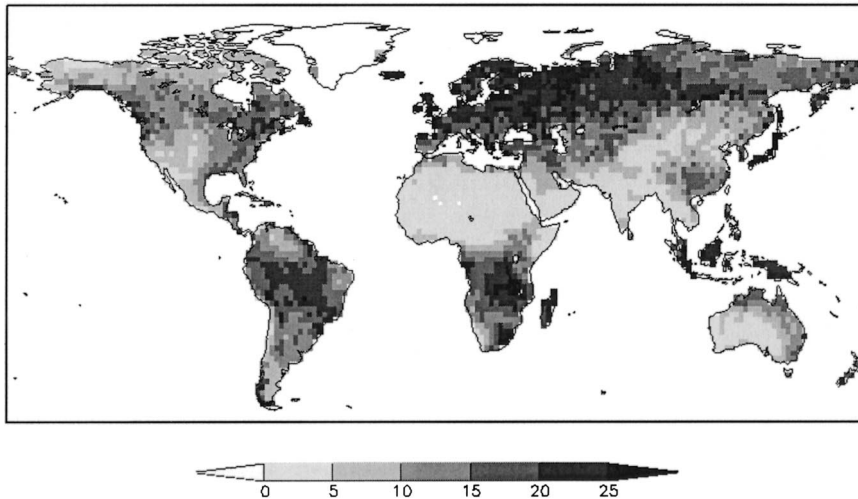


FIG. 5. Seasonally averaged monthly rain days for DJF over the period 1948–98 for the UW dataset and the NCEP dataset corrected with the UW monthly statistics.

dominates as in humid regions in summer months (New et al. 2000). The GPCP dataset relies on satellite data sources, which have much more uniform and consistent spatial coverage and may give better estimates at grid scales. The temporal extent of the dataset is also an important factor. A dataset with long temporal overlap with the NCEP dataset would likely provide a better representation of interannual variability and any trends over the 50-yr period than a mean monthly climatology based on fewer years. For the GPCP dataset (1997–99), the level to which the average monthly statistics are representative of the full time period (1948–98) is unknown. The CRU dataset may be more representative, by providing rain day frequencies and monthly totals for the whole time period, but it is of concern that

monthly conditional probability statistics had to be generated from the UW dataset. In the end, it may be that a hybrid of these datasets would provide the best estimate.

b. Loss of spatial coherence and storm tracking

Because the correction method is carried out individually for each grid cell, spatial coherence between neighboring cells may be lost. For example, during correction, the precipitation at one grid cell may be replaced with precipitation from a day chosen at random from the population of appropriate days (wet or dry). However, the precipitation in an adjacent cell may not be replaced with data from the same day, if it is replaced

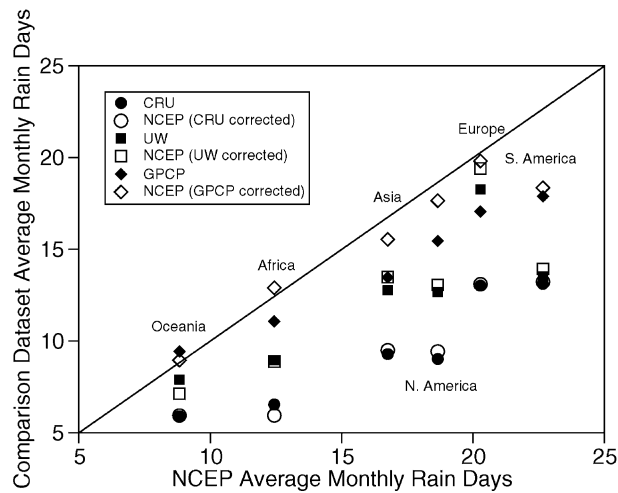


FIG. 6. Scatterplot of the NCEP average monthly number of rain days vs that for the comparison datasets (CRU, UW, and GPCP) (closed symbols) and the NCEP dataset corrected with each of the comparison datasets (open symbols) for the six continents.

at all, thereby losing spatial coherence between the two cells. For storm systems that span multiple grid cells, there may be a loss of spatial structure. Although this may not have major consequences on the mean precipitation over time and space scales larger than that of the storm, the effects at smaller spatial scales may be more profound. The passing of the storm over an area may be interrupted by the insertion of dry days into the continuous sequence of rain days. If the corrected dataset is to be used to force simulations of the land surface hydrology, this has potential effects on the dynamics of soil moisture and the occurrence of droughts and floods at the small scale. Figure 7 shows an example of the loss of storm tracking and spatial consistency for a sequence of four daily snapshots over North America. As large-scale weather systems move from west to east, their general features are retained in the corrected dataset but noise has been introduced. At the scale of an individual grid, the continuous sequence of rain days as a storm system passes over is disrupted by days of no precipitation. The opposite effect can occur over areas experiencing a period of dry weather.

c. Temporal persistence in related variables

The related meteorological variables are resampled for the same days as the precipitation to ensure consistency (section 4b). However, this may lead to a potential loss in the temporal persistence (lag-1 autocorrelation) in these variables because days are replaced at random without regard for the weather on preceding or following days. As an example, Table 1 shows the daily lag-1 autocorrelations averaged over 30° latitude bands for Asia for the NCEP dataset and the corrected dataset (using the CRU wet day frequencies). For both datasets, autocorrelations are lowest for precipitation and wind

speed, which is to be expected given the intermittent nature of storms and changes in wind speed at daily time scales. Values are high for most other variables, especially temperature, as they are dominated by the seasonal solar cycle, which tends to increase autocorrelation.

The reduced autocorrelation for precipitation in the corrected dataset is a result of the random sampling of wet days, which tends to break up multiday storms. As a result, the autocorrelation values for the other variables are also reduced in the corrected dataset but the extent to which this happens varies by type of variable and latitude band. Some of the largest differences occur in the Tropics for nearly all variables, and smaller differences are seen in higher latitudes. The exceptions to this are wind speed, which has significantly reduced autocorrelation in all regions, and surface pressure, which exhibits small differences in the Tropics due to the dominance of the Asian monsoon, and larger differences at higher latitudes where autocorrelations are less affected by the smaller seasonal variations.

Although it is apparent that there is a general loss in temporal persistence in all variables due to the correction, it is not clear whether the original NCEP lag-1 autocorrelations are realistic. As the NCEP dataset has incorrect autocorrelations because of the rain day problem, these will spill over into the other variables because of the correlation between them. Therefore, it can be argued that the correction method may reduce any autocorrelation bias in these variables while maintaining physical consistency among variables.

d. Effects on the land surface water budget

The motivation for correcting the NCEP precipitation is to generate long-term global fields of water and energy states and fluxes, which entails forcing state of the art land surface schemes with the best estimate of precipitation and surface meteorology available. The methods presented in this study combine observation-based global datasets with reanalysis datasets in order to obtain the best forcing dataset at the highest spatial and temporal scales possible. However, it is important to understand how the choice of dataset and methods used to construct such forcings affect the simulated land surface water budget. If the water budget is sensitive to the differences in these forcing datasets and the methods used to combine the data, then such simulations will only add to the uncertainty in our understanding of the land surface water cycle.

To examine this, a number of experiments were conducted by forcing the VIC land surface model (Nijssen et al. 2001a,b; Wood et al. 1997; Maurer et al. 2001) with each of the three corrected precipitation datasets, the NCEP dataset, and the NCEP dataset scaled to match the CRU monthly totals. These simulations are denoted as VIC_{CRU}, VIC_{UW}, VIC_{GPCP}, VIC_{NCEP}, and VIC_{NCEP-EP-SCALED}. In addition to precipitation, the VIC model

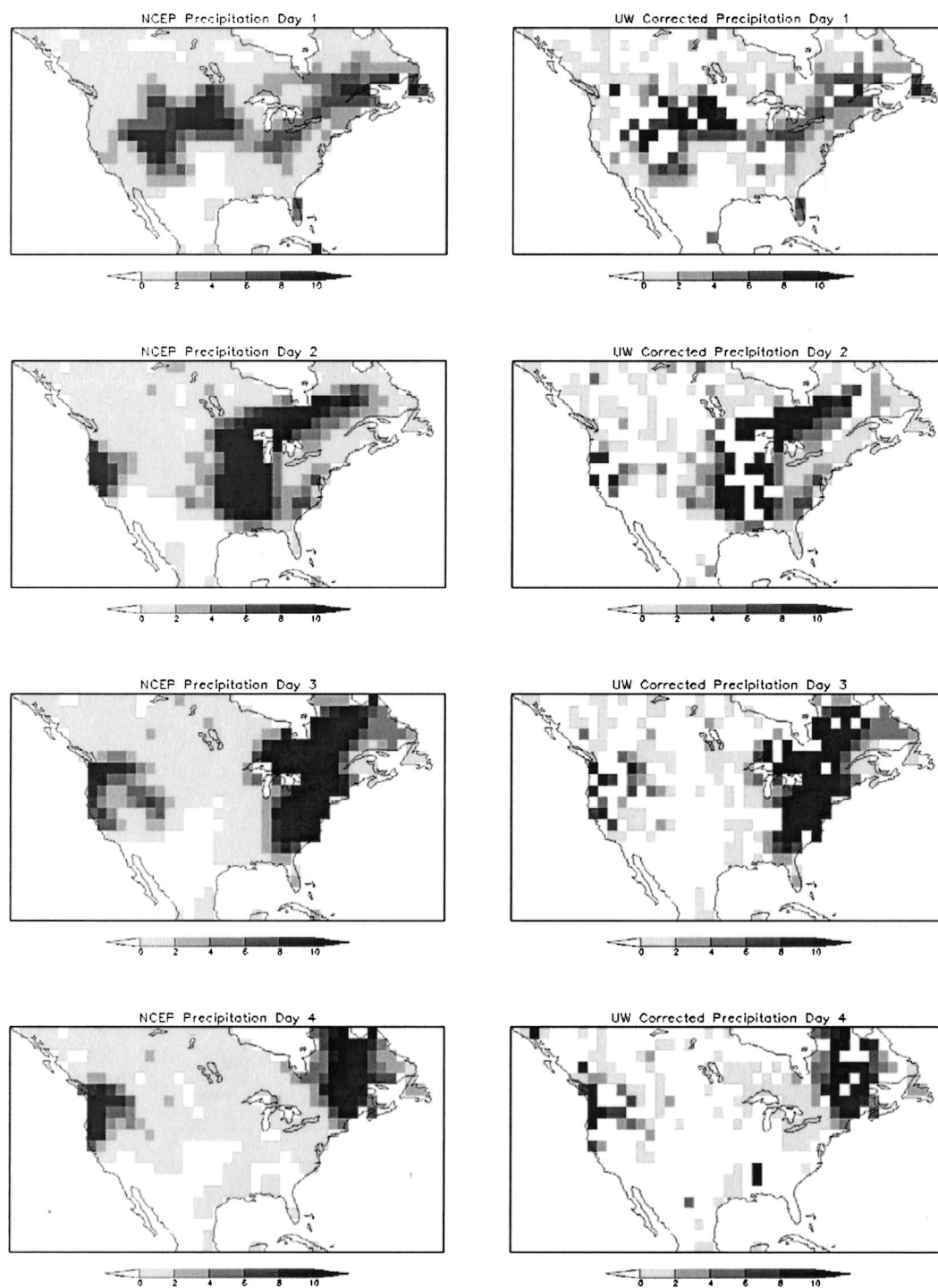


FIG. 7. A sequence of four daily precipitation (mm day^{-1}) maps for (a) the NCEP dataset and (b) the NCEP dataset corrected with the UW intermonthly statistics. Note the introduction of noise and the loss of storm tracking in the corrected dataset.

also requires, at the least, the daily maximum and minimum surface air temperature and wind speed, which were derived from the NCEP dataset and made consistent with the corrected precipitation as described in section 4c.

1) EFFECT OF THE NCEP HIGH-LATITUDE ANOMALY

Without correction of the biases and anomalies seen in the NCEP precipitation, the validity of using the

TABLE 1. Lag-1 autocorrelations for the NCEP dataset and the corrected dataset (using the CRU wet day frequencies). Autocorrelations are averaged over three latitude bands over Asia. Variables are precipitation (P), air temperature (T), downward shortwave radiation (SW), downward longwave radiation (LW), specific humidity (SH), surface pressure (P_s), and wind speed (W).

Dataset	P	T	SW	LW	SH	P_s	W
60°–90°							
NCEP	0.42	0.97	0.97	0.90	0.96	0.83	0.44
Corrected	0.16	0.89	0.94	0.80	0.86	0.41	0.22
30°–60°							
NCEP	0.45	0.97	0.91	0.91	0.93	0.84	0.45
Corrected	0.16	0.91	0.88	0.83	0.82	0.60	0.26
0°–30°							
NCEP	0.66	0.94	0.82	0.92	0.92	0.94	0.66
Corrected	0.23	0.84	0.65	0.79	0.76	0.81	0.44

NCEP dataset for land surface modeling in its native form is questionable. To illustrate this, an example of the effect of the high-latitude precipitation anomaly on the land surface hydrology is given in Fig. 8. This shows the average DJF snow water equivalent (SWE) for the VIC_{NCEP} simulation. This simulation was forced with the NCEP dataset in its raw form. The spurious pattern can clearly be seen in the SWE field in the high northern latitudes. Results for other land surface variables, such as evaporation, soil moisture content, and runoff (not shown), show little at these seasonal scales. This can be attributed to the fact that, at high latitudes in winter, the evaporation is very low and significant runoff and changes in soil moisture will not occur until the onset of spring melt, by which time the effects of the anomalous precipitation have begun to dissipate. The spurious pattern is of course not seen in the simulations forced with the corrected precipitation datasets.

2) EFFECT OF DIFFERENT RAIN DAY STATISTICS

The previous section showed that the land surface reflects the anomalies in the NCEP precipitation in its raw form and indicates that the correction to the rain day statistics is required to remove the effects of these biases. Therefore, it is important to determine the sensitivity of the land surface to the rain day statistics and to know the effect of the correction using rain day statistics from different datasets. In the context of large-scale modeling, the effects on the land surface budget at continental and global scales are of particular interest.

Table 2 shows the global and continental mean annual water budget for the VIC simulations. Also shown are the percentage changes in each of the budget components between each simulation and the VIC_{NCEP_SCALED} simulation. All simulations, except the VIC_{NCEP} simulation, are forced with precipitation scaled to match the monthly totals of the CRU dataset and this is reflected in the equal monthly precipitation totals in Table 2. The differences between the simulations show the effect of the choice of correcting dataset and are consistent with the comparison of rain day statistics shown previously in which, in general, the CRU dataset showed the largest differences with the NCEP dataset and the GPCP dataset showed the least.

The most notable effect on the land surface water budget is the way in which the precipitation is partitioned into evaporation and runoff. For all simulations forced with corrected precipitation, the evaporation is reduced and the excess water appears as a matching increase in runoff. The decrease in evaporation is mainly due to a decrease in canopy evaporation. For example, in North America, the evaporation for the VIC_{CRU} simulation is 28 mm lower than the VIC_{NCEP_SCALED} simulation and is matched by an increase of 28 mm in the

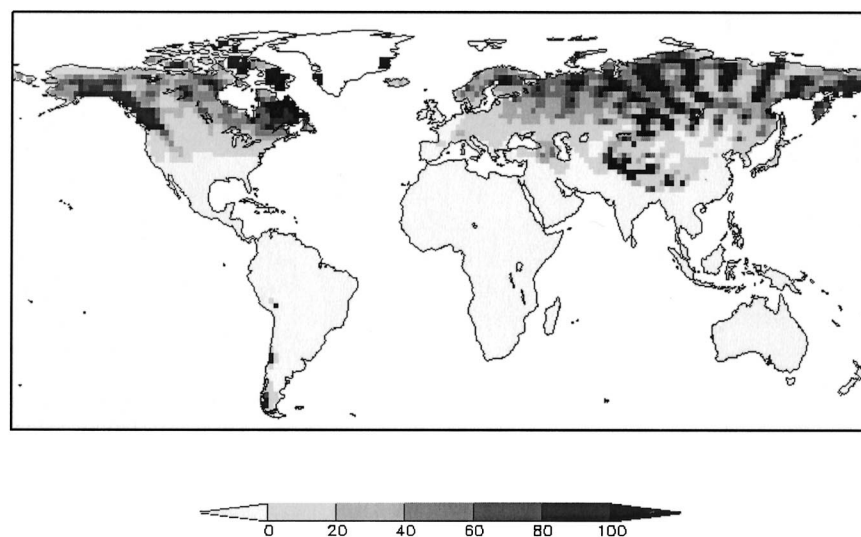


FIG. 8. Average DJF snow water equivalent (mm) for the VIC simulation forced by the NCEP precipitation.

TABLE 2. Global and continental mean annual hydrological budget for the VIC simulations forced with the NCEP dataset with scaled precipitation ($VIC_{NCEP,SCALED}$) and the three corrected datasets (VIC_{CRU} , VIC_{UW} , and VIC_{GPCP}). Water budget components are precipitation (P), evaporation (E), runoff (Q), soil moisture content (S), and snow water equivalent (SWE).

	$VIC_{NCEP,SCALED}$		VIC_{CRU}		VIC_{UW}		VIC_{GPCP}	
	Annual mean	Percent change	Annual mean	Percent change	Annual mean	Percent change	Annual mean	Percent change
P								
World	771	0.0	771	0.0	771	0.0	771	0.0
Africa	666	0.0	666	0.0	666	0.0	666	0.0
Asia	618	0.0	618	0.0	618	0.0	618	0.0
Europe	632	0.0	632	0.0	632	0.0	632	0.0
North America	668	0.0	668	0.0	668	0.0	668	0.0
Oceania	712	0.0	712	0.0	712	0.0	712	0.0
South America	1538	0.0	1538	0.0	1538	0.0	1538	0.0
E								
World	519	0.0	472	-9.1	484	-6.7	506	-2.5
Africa	562	0.0	523	-6.9	543	-3.4	555	-1.2
Asia	389	0.0	356	-8.5	375	-3.6	380	-2.3
Europe	494	0.0	479	-3.0	492	-0.4	492	-0.4
North America	447	0.0	419	-6.3	434	-2.9	444	-0.7
Oceania	483	0.0	460	-4.8	470	-2.7	480	-0.6
South America	870	0.0	726	-16.6	711	-18.3	813	-6.6
Q								
World	252	0.0	299	18.7	287	13.9	265	5.2
Africa	104	0.0	143	37.5	123	18.3	111	6.7
Asia	229	0.0	262	14.4	243	6.1	238	3.9
Europe	138	0.0	153	10.9	140	1.4	140	1.4
North America	221	0.0	249	12.7	234	5.9	224	1.4
Oceania	229	0.0	252	10.0	242	5.7	232	1.3
South America	668	0.0	812	21.6	827	23.8	725	8.5
S								
World	486	0.0	493	1.4	489	0.7	487	0.3
Africa	716	0.0	721	0.7	717	0.1	715	-0.1
Asia	391	0.0	397	1.5	394	0.7	394	0.6
Europe	659	0.0	664	0.8	662	0.5	661	0.3
North America	358	0.0	364	1.5	361	0.7	359	0.2
Oceania	347	0.0	356	2.5	351	1.1	348	0.3
South America	439	0.0	452	2.9	450	2.5	443	0.9
SWE								
World	20	0.0	17	-16.2	17	-14.3	19	-4.4
Africa	0	0.0	0	-11.6	0	-9.4	0	-5.3
Asia	22	0.0	18	-15.1	19	-12.2	21	-4.5
Europe	26	0.0	24	-6.4	25	-4.1	26	-0.3
North America	55	0.0	43	-20.7	45	-18.0	51	-6.3
Oceania	0	0.0	0	-8.3	0	-17.6	0	18.6
South America	4	0.0	5	10.5	4	-3.0	4	0.4

runoff. Canopy evaporation is lower by 101 mm and this is balanced by increases in transpiration (79 mm), soil evaporation (4 mm), soil moisture content (6 mm), and SWE (4 mm). The changes in snow sublimation and canopy storage are negligible.

Despite the monthly precipitation totals being equal for these simulations, the differences in the individual water budget components are quite large, especially in the partitioning of evaporation between canopy evaporation and transpiration. These differences can be explained by the differences in the monthly number of rain days and precipitation intensities. The NCEP data have less low-intensity precipitation and more high-intensity precipitation than the CRU- and UW-corrected

datasets. The fixed capacity of the vegetation canopy in the VIC model is exceeded by the more intense precipitation of the corrected datasets more often than for the NCEP dataset. The excess water is routed as throughfall to the soil surface, which reduces the amount of water available for canopy evaporation and increases the potential for surface and subsurface runoff and transpiration.

3) EFFECT OF LOSS OF SPATIAL COHERENCE

To determine the sensitivity of the land surface to the potential loss of spatial coherence in the corrected precipitation, spatial statistics were calculated over the Am-

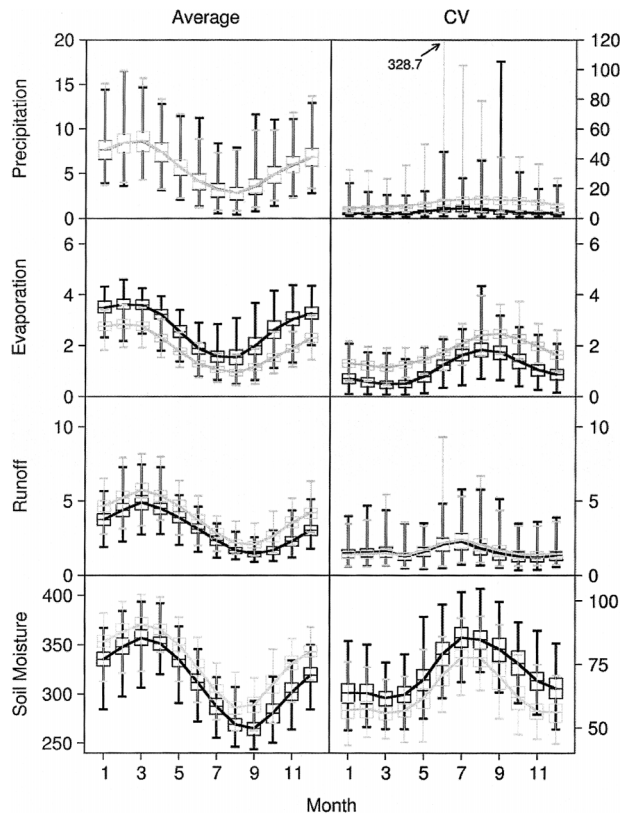


FIG. 9. Mean monthly time series of the distribution of the spatial average and CV of the main components of the land surface water budget over the Amazon River basin for the VIC_{NCEP_SCALED} (black line) and VIC_{CRU} simulations (gray line). The solid line represents the mean daily value. The upper and lower bars represent the maximum and minimum values, while the upper and lower limits of the boxes are the 75% and 25% quartiles. Units are mm day^{-1} for the fluxes and mm for the soil moisture. Note the different scales for the basin average and basin CV for precipitation and soil moisture.

Amazon River basin for the VIC_{NCEP_SCALED} and VIC_{CRU} simulations (see Fig. 9). This illustrates the effect of not only the differences in the rain day statistics but also how the loss of spatial coherence of precipitation occurrence affects the spatial variability of the land surface water budget. From Fig. 9, the basin-averaged precipitation is approximately the same for both simulations, which is to be expected, as the monthly precipitation totals are the same. Differences in the distribution of the daily basin-averaged values are due to changes made at the grid scale by the correction method. The CV values for precipitation for the two simulations show large differences. The mean coefficient of variance (CV) values for the VIC_{CRU} simulation are higher than those for the VIC_{NCEP_SCALED} simulation, as are, in general, the maximum and minimum values and the 25 and 75 percentiles. This is due to the breaking up of storm systems and the introduction of “noise” into the corrected precipitation dataset, which increases both the mean and the spread of the distribution of spatial variability.

Differences in basin-averaged evaporation are nota-

ble, with the mean VIC_{CRU} evaporation values being on average 21%–42% lower than for the VIC_{NCEP_SCALED} simulation. This is a result of the differential partitioning of precipitation into canopy evaporation and throughfall between the two simulations as was seen in the continental-scale analysis. Evaporation and runoff CV values tend to mimic the variability in the precipitation forcing, although the differences for runoff are small. Soil moisture CV values are high relative to the other components, which is to be expected at these spatial scales. However, any changes in variability resulting from changes in the spatial variability of precipitation are likely to be dampened because the soil moisture values are for the total active soil column, which includes deep moisture storage. Although the spatial variability in the VIC_{CRU} simulation precipitation is higher than for the VIC_{NCEP_SCALED} simulation, the corresponding variability in soil moisture is actually lower. This may be because the increased spatial variability in precipitation tends to produce a higher proportion of saturated or near-saturated soil moisture conditions across the basin and thus will reduce the spatial variability. This is more likely in a humid environment such as the Amazon River basin. The same analysis was carried out for the Mississippi and Mackenzie basins to investigate the effect for different climates and the results showed similar but smaller effects.

7. Summary and conclusions

A spurious wavelike pattern exists in the mean monthly precipitation and number of rain days of the NCEP dataset over terrestrial areas in high latitudes in winter. Comparison with the CRU, GPCP, and UW precipitation datasets verified the anomaly and other regional biases in the NCEP precipitation field. The rain day anomaly was corrected using the monthly precipitation statistics from each of the three comparison datasets and the resulting daily precipitation values were then scaled so that their monthly totals matched those of the CRU dataset. The monthly statistics of the resulting corrected datasets match well the statistics of the respective dataset used for the correction, but the degree to which it does this depends on the statistical similarity of the NCEP and correcting dataset.

In the context of land surface modeling, the need for the correction is clear, as the high-latitude anomalous pattern is reflected in the land surface states. A number of experiments were carried out to investigate the effect of the correction on the land surface by forcing the VIC land surface model with the original and corrected NCEP datasets. The results show that the land surface water budget is sensitive to the submonthly distribution of precipitation. Simulations forced with identical monthly precipitation totals but different rain day statistics can differ significantly in the partitioning of precipitation into canopy evaporation and throughfall with implications for the level of accuracy required of the

correcting dataset. Ultimately, the choice of the correcting dataset would be based on the level of confidence in the data and the accuracy of the rain day statistics at the grid scale. However, attention must also be paid to the temporal extent of the data and whether it is representative of the long-term variability over the multiple decades of the NCEP dataset period. In the absence of a single dataset that fulfills these criteria it may be that a hybrid dataset would have to be used.

A side effect of the correction method is that it introduces a degree of spatial inconsistency in the resultant precipitation fields because it is carried out independently for each grid cell. This results in the introduction of “noise” in the spatial pattern of precipitation and the potential loss of storm tracking at the regional scale. The spatial variability of water budget components appears to be sensitive to the increased spatial variability in the corrected precipitation field, at least over the scale of a large river basin such as the Amazon. The results for other basins indicate that there is less of an effect in cooler and drier climates. An important implication of this is for the simulation of the occurrence and magnitude of floods and droughts as the soil moisture field may develop very differently when forced with the corrected precipitation, not only because of the change in rain day statistics but also because the spatial structure of storms may be broken down. One potential solution to the problem of spatial incoherence is to use the method of correlated random numbers (Wilks 1998) although this is beyond the scope of this study. Nevertheless, for large-scale modeling, the side effects of the correction at continental and seasonal scales are small.

This work forms part of an effort to create a global, multidecade, daily, sub-2°, terrestrial, meteorological forcing dataset to drive land surface model simulations of the global water and energy balance. These simulations will provide a long-term, globally consistent and validated set of land surface water and energy fluxes and states at a high spatiotemporal resolution. The dataset will facilitate the study of seasonal and interannual variability studies to an extent not possible with currently available datasets. Furthermore, the dataset will be suitable for evaluating the ability of coupled models and other land surface prediction schemes to reproduce observed variability of surface fluxes and state variables in space, and temporally for time scales up to decadal. In addition, this long-term dataset will be useful for diagnostic studies related to terrestrial hydrology, and for intercomparison studies with numerical weather prediction (NWP) reanalysis datasets.

Acknowledgments. This work was funded by NASA Grant NAG5-9414. The GPCP data were provided by the Global Precipitation Climatology Center (GPCC) from their Web site (<http://www.dwd.de/research/gpcc>; downloaded November 2000). NCEP–NCAR reanalysis data were provided by the NOAA–CIRES Climate Di-

agnostics Center, Boulder, Colorado, from their Web site (<http://www.cdc.noaa.gov/>; downloaded November 2000). The CRU data were created and supplied by Dr. Mike Hulme at the Climatic Research Unit, University of East Anglia (UK) (provided January 2001). The UW data were provided by the Surface Water Modeling group at the University of Washington.

REFERENCES

- Cullather, R. I., D. H. Bromwich, and M. C. Serreze, 2000: The atmospheric hydrologic cycle over the Arctic Basin from re-analyses. Part I: Comparison with observations and previous studies. *J. Climate*, **13**, 923–937.
- Gibson, J. K., P. Kallberg, S. Uppala, A. Hernandez, A. Normura, and E. Serrano, 1997: ERA description. ECMWF Re-Analysis Project Report Series 1, ECMWF, Reading, United Kingdom, 72 pp.
- Huffman, G. J., and Coauthors, 1997: The Global Precipitation Climatology Project (GPCP) combined precipitation dataset. *Bull. Amer. Meteor. Soc.*, **78**, 5–20.
- , R. F. Adler, M. M. Morrissey, D. T. Bolvin, S. Curtis, R. Joyce, B. McGavock, and J. Susskind, 2001: Global precipitation at one-degree daily resolution from multisatellite observations. *J. Hydrometeorol.*, **2**, 36–50.
- Hulme, M., 1995: Estimating global changes in precipitation. *Weather*, **50**, 34–42.
- Janowiak, J. E., A. Gruber, C. R. Kondragunta, R. E. Livezey, and G. J. Huffman, 1998: A comparison of the NCEP–NCAR reanalysis precipitation and the GPCP rain gauge–satellite combined dataset with observational error considerations. *J. Climate*, **11**, 2960–2979.
- Kalnay, E., and Coauthors, 1996: The NCEP/NCAR 40-Year Reanalysis Project. *Bull. Amer. Meteor. Soc.*, **77**, 437–471.
- Kanamitsu, M., W. Ebisuzaki, J. Woollen, S.-H. Yang, J. J. Hnilo, M. Fiorino, and G. L. Potter, 2002: NCEP–DOE AMIP-II Reanalysis (R-2). *Bull. Amer. Meteor. Soc.*, **83**, 1631–1643.
- Kistler, R., and Coauthors, 2001: The NCEP–NCAR 50-Year Reanalysis: Monthly means CD-ROM and documentation. *Bull. Amer. Meteor. Soc.*, **82**, 247–268.
- Maurer, E. P., G. M. O’Donnell, D. P. Lettenmaier, and J. O. Roads, 2001: Evaluation of NCEP/NCAR reanalysis water and energy budgets using macroscale hydrologic simulations. *Land Surface Hydrology, Meteorology, and Climate: Observations and Modeling*, Amer. Geophys. Union Series in Water Science and Applications, V. Lakshmi, J. Albertson, and J. Schaake, Eds., Vol. 3, 137–158.
- New, M. G., M. Hulme, and P. D. Jones, 1999: Representing twentieth-century space–time climate variability. Part I: Development of a 1961–90 mean monthly terrestrial climatology. *J. Climate*, **12**, 829–856.
- , —, and —, 2000: Representing twentieth-century space–time climate variability. Part II: Development of 1901–96 monthly grids of terrestrial surface climate. *J. Climate*, **13**, 2217–2238.
- Nijssen, B., G. M. O’Donnell, D. P. Lettenmaier, D. Lohmann, and E. F. Wood, 2001a: Predicting the discharge of global rivers. *J. Climate*, **14**, 3307–3323.
- , R. Schnur, and D. P. Lettenmaier, 2001b: Global retrospective estimation of soil moisture using the Variable Infiltration Capacity land surface model, 1980–93. *J. Climate*, **14**, 1790–1808.
- Serreze, M. C., and C. M. Hurst, 2000: Representation of mean Arctic precipitation from NCEP–NCAR and ERA reanalyses. *J. Climate*, **13**, 182–201.
- Susskind, J., P. Piraino, L. Rokke, L. Iredell, and A. Mehta, 1997: Characteristics of the TOVS Pathfinder Path A Dataset. *Bull. Amer. Meteor. Soc.*, **78**, 1449–1472.
- Trenberth, K. E., and C. J. Guillemot, 1998: Evaluation of the atmospheric moisture and hydrological cycle in the NCEP/NCAR reanalysis. *Climate Dyn.*, **14**, 213–231.

- WCRP, 1990: The Global Precipitation Climatology Project—Implementation and data management plan. WMO Tech. Doc. 367, Geneva, Switzerland, 47 pp. and appendixes.
- Wilks, D. D., 1998: Multi-site generalizations of a daily stochastic weather generation model. *J. Hydrol.*, **210**, 178–191.
- , and R. L. Wilby, 1999: The weather generation game: A review of stochastic weather models. *Prog. Phys. Geogr.*, **23**, 329–357.
- Wood, E. F., D. P. Lettenmaier, X. Liang, B. Nijssen, and S. W. Wetzel, 1997: Hydrological modeling of continental-scale basins. *Annu. Rev. Earth. Planet. Sci.*, **25**, 279–300.